Modeling of Pilot-Scale Saltcake Dissolution

R.K. Toghiani, L.T. Smith, J.S. Lindner
Diagnostic Instrumentation and Analysis Laboratory
Mississippi State University
205 Research Blvd, Starkville, MS, 39759
USA

G.I. Tachiev, G. Yaari
Applied Research Center
Florida International University
10555 West Flagler St, EC 2100, Miami, FL, 33174
USA

ABSTRACT

Large portions of the high-level waste present at the Hanford Site and Savannah River Site are comprised of porous salts with associated interstitial liquors. Various processes have been proposed wherein the aqueous phase is removed followed by dissolution of the salt with further mixing or blending of the resulting stream in a receiver tank. This leads to a large reduction in the radioactivity for the dissolved saltcake; however, the interstitial retrieval process is hindered by capillary forces within the saltcake pores and large aqueous phase fractions may remain. Thus, the interim stabilized or low-curie salt processes may have less separation effectiveness than desired. In addition, based on the initial extent of pretreatment of the waste, the saltcake may be either unsaturated or hydraulically saturated. Different interactions are expected based on the contact of the diluent with the salt and/or on mixing the diluent with the salt and some fraction of interstitial liquid. The initial approximation is that the dissolution is governed by the associated thermodynamics of the system. This may be correct assuming sufficient time for contact between the salt and diluent has occurred. Pilot-scale simulant saltcake dissolution experiments have been conducted by the Applied Research Center (ARC) at Florida International University. As part of a companion program, these experiments have been modeled at the Diagnostic Instrumentation and Analysis Laboratory (DIAL, Mississippi State University) using the Environmental Simulation Program (ESP, OLI Systems, Inc.). Hanford simulant compositions were examined under unsaturated and saturated conditions. To account for channeling that occurred during the unsaturated experiment, additional operations were required for the process flowsheet. Direct modeling of the saturated bed was possible without this consideration. The results have impacts on the saltcake retrieval process. First, depending on the extent of interstitial liquid contained in the waste, recycling may be necessary; removal of the resulting aqueous stream at the largest specific gravity consistent with the operating safety basis ensures productive use of water. Secondly, direct modeling of a given waste dissolution must consider variations in the extent of channeling such that limits can be established on anticipated concentrations expected during the course of the retrieval. Finally, the ability to account for heterogeneous dissolution has been accounted for. Details regarding the development of the modeling strategy as well as knowledge gained regarding flowsheet development are provided.

INTRODUCTION

The Hanford site contains approximately 53 million gallons of waste stored in 177 underground storage tanks [1]. A total of 149 single-shell tanks (SSTs) and 28 double-shell tanks (DSTs) are located in a number of tank farms. The SST's contain the bulk of the salt waste while the DSTs predominately contain sludge and interstitial liquor. A recent effort to drain the interstitial liquor from the SST's, known as the interim stabilization program, has been completed. This has allowed for a coarse separation of the Cs-137 from the salt waste and has also minimized the potential for leakage from the SSTs.

The predominant salt in the waste is sodium nitrate, resulting from the caustic neutralization of nitric acid employed in nuclear material processing. A number of different processes were employed at the site leading to formation of additional salts containing phosphate and sulfate. Carbonate salts are present owing to the solubility of CO_2 in highly alkaline (pH >14) wastes. The overall composition of the salt wastes is provided in Table I [2].

Table I. Primary Constituents in the Hanford SST's [2]

Component	Weight (kg)	Weight (%)
Al^{3+}	2.4×10^{6}	1.3
Na^{+}	5.2×10^{7}	27.9
NO_2^{-}	4.8×10^{6}	2.6
NO_3^{-}	9.6×10^{7}	52.2
OH^{-}	9.1×10^{6}	4.9
Other	2.0×10^{7}	11.0
Total	1.8×10^{8}	100.0

Current waste processing operations rely on the separation of the waste into high and low radioactivity streams. The high level waste will be vitrified in the Waste Treatment Plant (WTP) while the low level waste will be processed into a stable waste form at the WTP facility or processed using bulk vitrification [3, 4]. The ability to separate the waste into high and low radioactivity fractions will depend on: 1) the composition of the retrieved streams from dissolution of the salt; 2) the routing of the waste; and 3) any pretreatment operations, such as fractional crystallization or ion exchange, that may be employed.

Small-scale, laboratory-based studies on saltcake dissolution have been reported previously by Herting [5]. These efforts were designed to obtain information on the partitioning of the salts into the solid and liquid phases as diluent was added. At the same time, work began at DIAL on thermodynamic modeling of the dissolution process [6]. Calculations were performed using ESP. The overriding goal of these simulations was model validation through direct comparisons with the experimentally determined ion concentrations and solids identification. Comparisons were also made with solubility data from the literature, especially for double salts, such as $Na_7FPO_4{\cdot}19H_2O$, Na_3FSO_4, and $Na_6(SO_4)_2CO_3$, that had been identified in Hanford salt waste. Pertinent thermodynamic data for many of these systems were limited and often available only in aqueous solution; consequently, a series of solubility studies were initiated with emphasis on conditions relevant to the Hanford site. The resulting data, along with well established interaction parameters, were subsequently used to develop a specific compilation, the double salt database (DBLSLTDB), that is directly applicable to high pH alkaline wastes. Further refinements and additions to DBLSLTDB have continued as have additional comparisons to the saltcake dissolution process associated with both Hanford and the Savannah River Site [7, 8].

All of the experiments performed by Herting were conducted at the laboratory scale where perfect mixing of the diluent with the interstitial liquid and the salts was achieved. In practice, however, the extent of mixing within a waste tank will be dependent on the heterogeneity of the waste as well as on the ability to disperse the diluent to contact all of the waste in the tank. The waste heterogeneity complicates the dissolution process in that some salts have greater solubility than others. Layers of hard-to-dissolve solids, such as sodium oxalate, will limit the movement of the dilution water through the bed due to decreased saltcake permeability.
In order to more fully evaluate the extent of mixing during the saltcake dissolution process and to provide further data for model validation and flowsheet development, workers at ARC have performed pilot-scale experiments [9, 10] on simulant compositions derived from Hanford waste inventories for saltcakes in tanks S-112 and S-109 [11, 12]. The experiments included the preparation of the given saltcake, transfer of the simulant to a 25.4 x 254 cm tall column, draining of the interstitial liquid, adding diluent and collecting aqueous fractions as a function of the extent of dissolution. For the S-112 experiment, extensive draining of the interstitial liquor was performed leading to an experiment representative of an unsaturated waste hydrology. For the S-109 experiment, the interstitial liquid was recycled from the bottom to the top of the column multiple times to establish the saltcake column. The liquid was then drained such that the liquid surface was at the same height as the saltcake bed. This experiment was representative of a saturated waste hydrology. The two experiments represent the extremes with respect to the hydrology and encompass the limits anticipated within Hanford waste tanks.
In this work, details of the ESP calculations are given and the predictions are compared to the ARC experimental results. Practical options for modeling saltcake waste retrievals have been identified.

ESP MODELING

Two different versions (6.5 and 6.7) of ESP were used for the simulations of S-112 and S-109 simulant dissolution, respectively. In both cases, the DBLSLTDB was employed. In this regard, however, it should be noted that OLI Systems, Inc., upgrades their Public database with the release of a new version; consequently, data regressions contained in the DBLSLTDB database were re-evaluated with the move from ESP 6.5 to ESP 6.7 to ensure consistency in predictions with the solubility experiments performed at DIAL and with the available literature data.
ESP employs the principle of Gibbs Energy minimization to partition the species present between their aqueous phase constituents and their solid phase constituents. Defining the chemistry for the particular problem requires input of the various chemical species in the simulant recipe. The chemistry model, accounting for all chemical equilibrium reactions that may possibly occur between the various species, is generated within the software. Modules within the program are then selected to evaluate mass and energy balances for the various unit operations present in the process flowsheet.

Model Predictions for the S-112 Unsaturated Experiment

For the S-112 unsaturated hydrology experiments, four separate batch compositions were prepared by workers at ARC [9]. Each batch was prepared using the same initial amount of each chemical, but the extent of evaporation of water from the slurry was different for each batch. For example, each batch contained approximately 122 kg water. However, for Batches 1 and 2,

approximately 47% of the water was evaporated from each batch, while for Batches 3 and 4, approximately 75% of the water was evaporated from each batch. This resulted in much higher concentrations of aqueous phase constitutions in Batches 3 and 4 as compared to Batches 1 and 2. ESP model predictions for the aqueous phase concentrations for the various species as well as the physical properties for the liquid phase are shown in Table II. All concentrations are in moles/L. Also notable are the increased liquid phase densities for Batches 3 and 4 as compared to Batches 1 and 2. Fewer solids were formed upon cooling of Batches 1 and 2, while more solids were formed upon cooling of Batches 3 and 4, as indicated in Table III. For Batches 1 and 2, no sodium nitrate, sodium carbonate monohydrate, or sodium sulfate were predicted to be present in the solid phase. For Batches 3 and 4, these three species accounted for greater than 50% (by weight) of the solids formed. The last column in Table III lists the solids formed upon mixing of the aqueous phases of the four batches.

Table II. ESP Predictions for the Aqueous Phase of the ARC Batch Preparations

Concentration (M)	Batch 1	Batch 2	Batch 3	Batch 4
Al^{+3}	0.15	0.13	0.41	0.59
Cl^{-}	0.12	0.12	0.20	0.31
CO_3^{-2}	0.24	0.22	0.34	0.29
F^{-}	9.77E-04	1.02E-03	8.65E-04	9.93E-04
Na^{+}	8.54	8.10	10.17	9.91
NO_2^{-}	0.33	0.31	0.58	0.87
NO_3^{-}	4.28	4.05	4.87	4.13
OH^{-}	0.97	0.93	1.43	2.22
$C_2O_4^{-2}$	3.89E-03	4.42E-03	1.84E-03	1.09E-03
PO_4^{-3}	3.74E-02	4.20E-02	1.80E-02	1.01E-02
SO_4^{-2}	0.27	0.26	0.28	0.17
Total Mass (kg)	108.35	109.21	67.77	43.44
Volume (L)	76.92	78.69	45.87	29.99
Density (g/L)	1408.64	1387.92	1477.46	1448.58
Abs Viscosity (cP)	6.44	5.78	9.99	9.58
pH	14.70	14.61	15.23	15.42
Ionic Strength	11.73	10.96	14.39	13.51

An initial attempt (Attempt #1) to model the column dissolution experiment by sequentially adding batches 1-4, accounting for the 168L of brine that were removed from the column as the saltcake settled, and then adding diluent yielded unrealistic results. Table IV shows the predicted simulation results for a saltcake prepared in this manner and compares it to the final saltcake composition used in the dissolution simulations. This latter composition (Attempt #2) was arrived at by separating the solid phase and aqueous phase for each batch from one another, then mixing all of the aqueous streams together, resulting in the reprecipitation of a small amount of solids. The combined aqueous stream was then split to account for the 168 L

Table III. ESP predictions for Solids Formation

Stream	Batch 1	Batch 2	Batch 3	Batch 4	Reprecipitated Solids[a]
Solid (kg)					
$Al(OH)_3$	2.26	2.28	1.64	1.74	0.56
$Na_2C_2O_4$	1.08	1.04	1.09	1.10	0.01
$Na_2CO_3 \cdot H_2O$			3.53	6.80	
Na_2SO_4			1.11	2.20	
$Na_7F(PO_4)_2 \cdot 19H_2O$	0.71	0.68	0.72	0.73	
$NaNO_3$			8.53	17.01	
$Na_3PO_4 \cdot 12H_2O \cdot 0.25NaOH$	6.24	5.83	6.89	7.09	0.32
Total Mass (kg)	10.28	9.82	23.51	36.67	0.90
Volume (L)	5.60	5.33	11.85	17.98	0.44
Density (g/L)	1835.27	1844.12	1982.80	2039.93	2056.22

[a] solids formed upon mixing of aqueous phase obtained from all batches

of brine drained from the column while the re-precipitated solids were added to the original solids formed. The solid phase and the aqueous phase for the starting composition were treated separately in the process flowsheet.

In Attempt #1 all of the prepared batches were simply combined, and as a result, the total amount of solids and solid phase speciation changed. The nitrate anion loadings in the initial batch preparations are all less than 5 M (Table II) and below saturation. When the high sodium nitrate solids streams in Batches 3 and 4 were mixed with Batches 1 and 2, the higher water loadings and lower ionic strengths of Batches 1 and 2 favored dissolution of solid sodium nitrate. Other changes were also evident including the dissolution of sodium sulfate and the reduced mass of solid sodium carbonate monohydrate. This loss of solids led to a low value for the solid volume fraction, V2. Assuming that the solids have a porosity of 100%, a layer of free liquid of approximately (78 L - 22 L), or 56 L, would result. The total height of this volume within the 13-inch column would be 26 inches and this result is inconsistent with images collected prior to the addition of diluent [9].

On the other hand, treating the aqueous phase and solids separately (Attempt #2), implying a lack of mixing between the phases, resulted in ion concentrations that were in good agreement with the ARC measurements (averages taken from Table 20 of reference 9). The ESP prediction for the average aluminum concentration was lower than that measured while the nitrate ion concentration was somewhat higher. The predicted aluminum concentration being lower than the experimental value is expected as ESP predicts that aluminum is partitioned into the solid phase as gibbsite, without regard to the slow kinetics associated with gibbsite formation. The fraction of ions removed during the draining of the 168 L is compared to the ARC mass balance in Table V. The results are consistent with the differences in concentrations given in Table IV.

Process Flowsheets

All of the calculation strategies were designed to separately treat the solids and the brine. The first process is illustrated in the flowsheet identified as FS#1 in Fig. 1. In this flowsheet, it was assumed that all of the diluent only interacted directly with the solids resulting in a dissolved salt solution, which was then mixed with the brine. The combined brine stream was then split to account for the volume of the fraction collected. The remaining solids and the

Table IV. ESP Predictions for Saltcake Preparation

Aqueous[a]	ESP Attempt #1	ESP Attempt #2	ARC Avg. [9]	ARC Std. [9]
H_2O (mol)	3286.56	2783.32		
Al^{+3}	0.34	0.22	0.36	0.07
Cl^-	0.15	0.16	0.19	0.11
CO_3^{-2}	0.36	1.04	NA[b]	
F^-	7.97E-04	9.75E-04	2.00E-03	
Na^+	10.37	8.90	8.88	0.43
NO_2^-	0.26	0.28	0.28	0.05
NO_3^-	5.23	4.21	3.97	0.30
OH^-	1.03	1.24		
$C_2O_4^{-2}$	2.33E-03	2.94E-03	3.00E-03	1.41E-03
PO_4^{-3}	2.46E-02	2.81E-02	3.86E-02	8.00E-03
SO_4^{-2}	0.33	0.25	0.20	0.06
Total Mass (kg)	117.717	8.93E+01		
Volume (L)	78.7401	62.86		
Density (g/L)	1495	1420.25		
Abs. Viscosity (cP)	10.1717	7.14		
pH	15.1176	14.90		
Ionic Strength	15.0407	12.21		
Solids (kg)				
$Al(OH)_3$	5.89	8.48		
$Na_2C_2O_4$	4.34	4.32		
$Na_2CO_3 \cdot H_2O$	0.14	10.33		
Na_2SO_4		3.31		
$Na_7F(PO_4)_2 \cdot 19H_2O$	2.85	2.83		
$NaNO_3$	0.44	25.54		
$Na_3PO_4 \cdot 12H_2O \cdot 0.25NaOH$	26.51	26.37		
Total (kg)	40.16	81.17		
Volume (L)	22.35	41.19		
Density (g/L)	1797.20	1970.49		
Total Stream				
Mass (kg)	157.88	170.47		
Volume (L)	101.09	104.06		
% Solids by weight	25.44	47.62		
V1	0.78	0.60		
V2	0.22	0.40		
% Water by weight	29.41	29.41		

[a] ion concentrations in moles/L

[b] experimental result not reported

reprecipitated solids from the brine mixing operation were then mixed with the second diluent addition and the process repeated.

As described below, the initial flowsheet led to large differences between the predicted and experimental effluent concentrations. Consequently, a revised flowsheet, given as FS#2 in Fig. 1, was developed in an attempt to explain the partitioning of the diluent between solids dissolution and brine dilution.

Table V. Percentage of Ions Removed Prior to the Start of Diluent Addition

Ion	ESP	ARC [9]
Al^{+3}	23	31
Cl^{-}	73	59
CO_3^{-2}	54	n.a.(1)
F^{-}	4	7
Na^{+}	55	54
NO_2^{-}	73	61
NO_3^{-}	55	53
OH^{-}	73	n.a.(1)
$C_2O_4^{-2}$	2	1
PO_4^{-3}	6	7
SO_4^{-3}	54	52

(1) particular anion was not determined in analysis

For approximately 27 days, diluent at a flow rate of 4 cc/min was added to the column. Volumes of the fractions collected are provided in reference 9 and these along with the total volume of brine were used to set the volume of the fractions recovered.

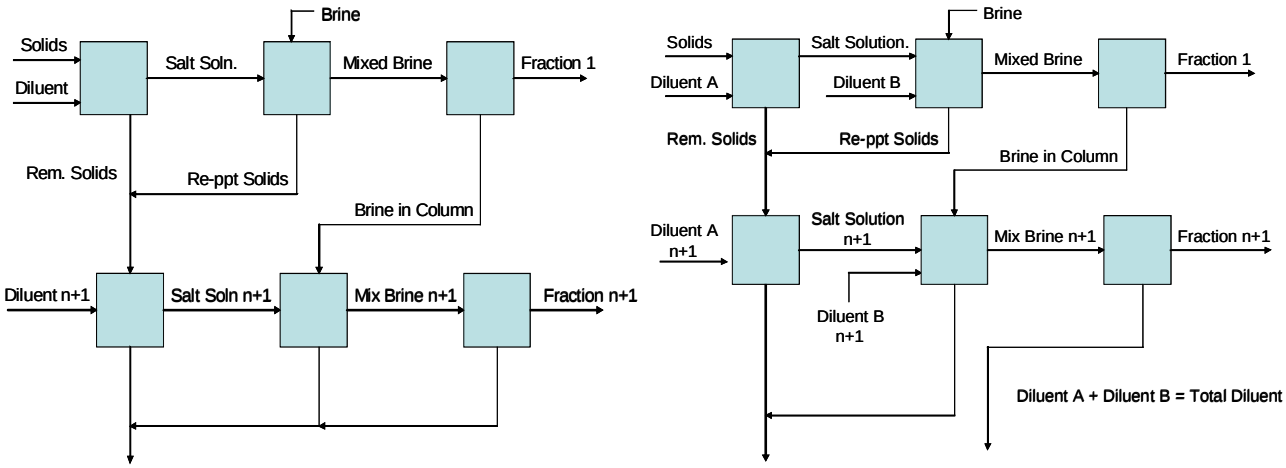

FS#1 FS#2

Fig. 1. ESP flowsheets employed for the unsaturated S-112 simulant pilot-scale dissolution experiment conducted at ARC

Process Modeling using the Solids Only Dissolution Model

Calculations using the FS#1 flowsheet were carried out and compared with experimental results for the first six days of the experiment. Initial simulations were aimed at observing the typical

expectations for saltcake dissolution as compared to the experimental results. Upon addition of diluent water to the saltcake, it is expected that those solids with large solubilities, such as $NaNO_3$ and $Na_2CO_3.H_2O$ will tend to dissolve first, followed by the double salts and then salts with very limited solubility such as $Na_2C_2O_4$. This behavior has been observed in previous studies [5-8]. Ions that would typically remain in the aqueous phase include chloride, hydroxide, nitrite and Cs-137. Thus, these constituents would strictly undergo dilution as the interstitial liquor was mixed with the diluent water. On the addition of the diluent water, the salts dissolve, increasing the density of the aqueous phase and increasing the ionic strength. Solid dissolution leads to an initial increase in ion concentration. Once a solid species has been entirely dissolved, the corresponding ion concentrations will decrease exponentially as a function of diluent addition. This behavior is observed in Fig. 2. However, there are a number of other factors that affect the results. Fig. 2 contains the experimental concentrations (moles/L) for Na^+, NO_3^-, NO_2^-, and the aqueous phase density (kg/L) as well as the predictions from both flowsheets, FS#1 and FS#2.

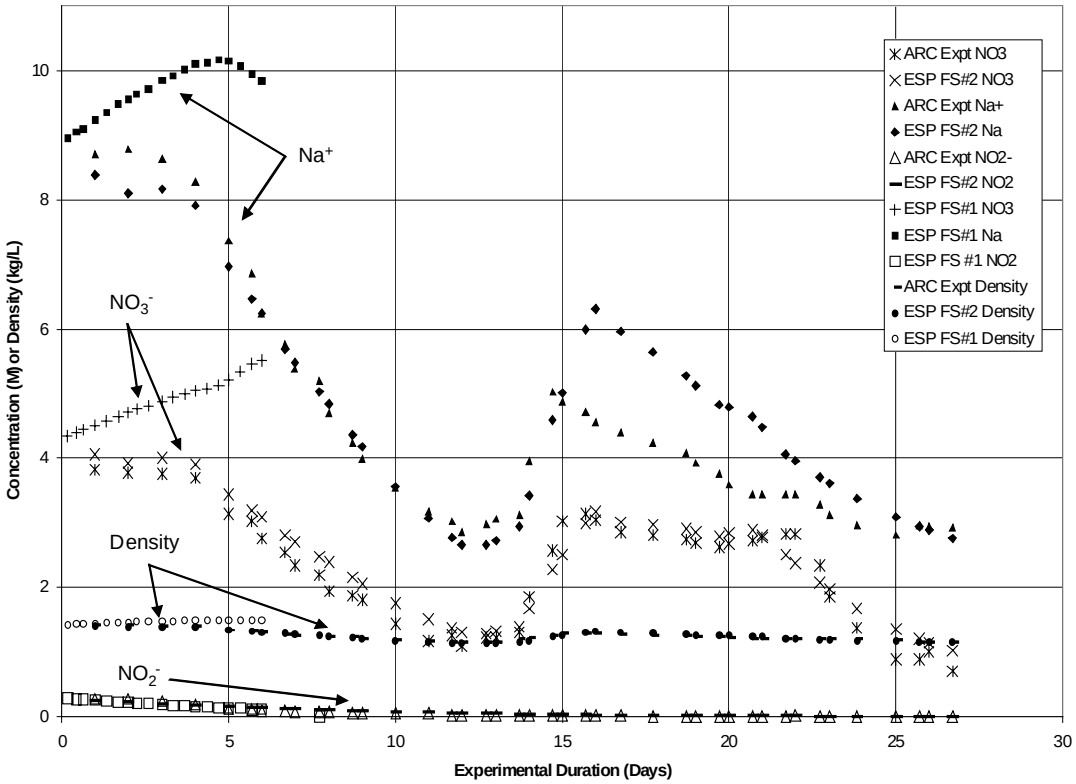

Fig. 2. Comparison of ESP model predictions for flowsheets FS#1 and FS#2 and experimental data

Simulations for flowsheet FS#1 were performed only for the first 6 days of the experimental run. The nitrite ion concentration decreased as diluent is added and this is consistent with the absence of any solid sodium nitrite in the saltcake.

Comparison of the experimental results for Na^+ and NO_3^- as well as the liquid phase density indicated that the model predictions increased in all cases whereas, the experimental results either increased slightly or stayed constant as the diluent was added. Further examination of the

experimental results indicated a gradual decrease in the sodium and nitrate ion concentrations followed by an increase around 15 days into the experimental run. The density follows a similar trend, which is inconsistent with the general behavior of salts during dissolution when complete mixing between the diluent and the solid phase is assumed. Consequently, flowsheet FS#1 was modified, giving rise to flowsheet FS#2, where the diluent water was partitioned between dissolving the solid phase and diluting the salt supernatant that was formed upon dissolution. From a practical standpoint, this represents channeling of the diluent away from the solids implying the existence of large pores within the salt matrix and the diluent water not having sufficient time to interact with the salt.

The agreement between the model predictions and the experimental results was much better using flowsheet FS#2. In this case, the known nitrate concentrations were used recursively to partition the water between the solid phase and the dissolved salt solution. Clearly, for an actual salt waste retrieval from a million gallon storage tank, such an approach would not be practical. However, the distribution of the diluent can be approximated.

The resulting percentage of water that is routed for dilution of the brine along with the predicted liquid and solid volume fractions, V1 and V2, are given in Fig. 3. Periods where the diluent is strongly interacting with the available brine have been denoted as periods when extensive channeling occurs. With the exception of the volume fractions at day 10, the value of V1 is always greater than V2. Both V1 and V2 are nearly constant during the initial portion of the experiment. Once solid dissolution begins, a gradual decrease in V2 and an increase in V1 occurs.

Agreement of the experimental and calculated nitrate ion was expected based on the use of the nitrate concentrations for recursion. Additional data for aluminum, chloride, and oxalate are given in Table VI. The chloride tends to remain in the aqueous phase and both the experimental results and the model predictions indicate a decay owing to dilution. In practice, aluminum is partitioned between $Al(OH)_4^-$ and gibbsite ($Al(OH)_3$) [13]. The small aluminate concentration in the aqueous phase undergoes dilution, but gibbsite can only be dissolved under these conditions by increasing the hydroxide loading. In the case of the insoluble salt, sodium oxalate, the dissolution is delayed. Concentrations of the $C_2O_4^{-2}$ ion are near the experimental detection limit at the beginning of the experiment and then slowly increase as dilution proceeds.

The water function describing the partitioning of the diluent between solids dissolution and brine dilution developed for flowsheet FS#2 is unique to the experiment. It is believed that, in most practical tank farm operations, functions approximating those in Fig. 3 would not be applicable. This specifically relates to the HNF interim stabilization process or the SRS low-curie salt process where, for different reasons, the vast majority of the interstitial liquor has already been removed. In those tanks where large volumes of interstitial/free liquid are present, the approach used in flowsheet FS#2 is expected to be useful in bracketing the expected effluent concentrations. Workers at Hanford are planning on installing an on-line Raman spectroscopy system for the quantitation of anion and cation concentrations of the resulting salt solutions as they are transferred to the DST tank farm [14]. The approach described, coupled with the experimental results from the Raman system, could provide engineers at the site with additional

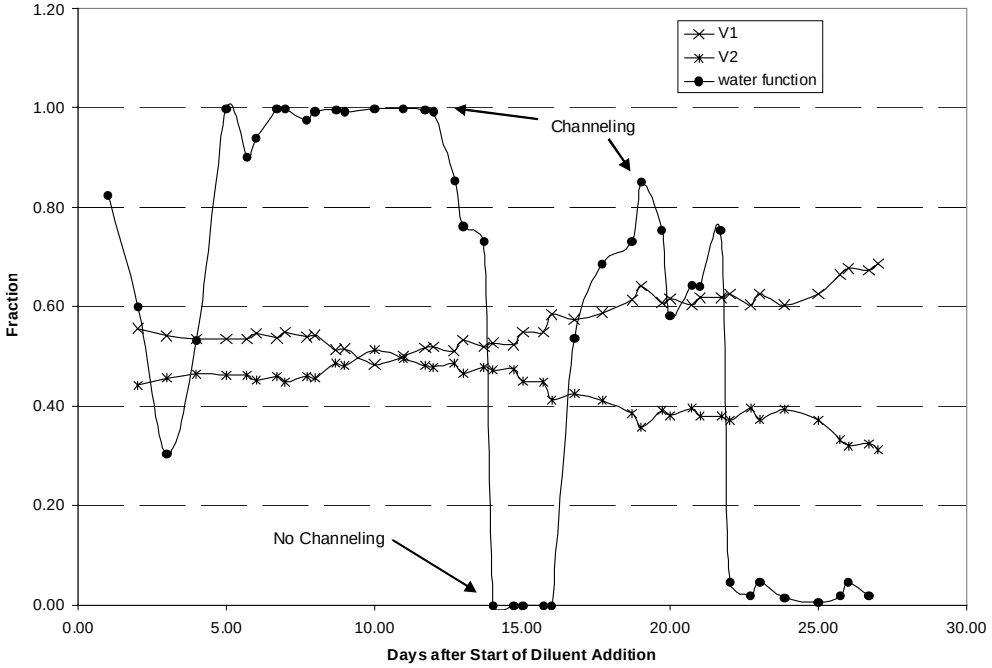

Fig. 3. Partitioning of diluent water between the solid phase and dilution of the dissolved salt solution

Table VI. Comparison of Select Ion Concentration Predictions Using Flowsheet FS#2 and Experimental Data (all values are in mole/L)

Day[a]	Expt Al^{+3} [9]	ESP Al^{+3}	Expt Cl^- [9]	ESP Cl^-	Expt $C_2O_4^{-2}$ [9]	ESP $C_2O_4^{-2}$
1.0	3.38E-01	1.74E-01	1.81E-01	1.48E-01	0.00E+00	2.77E-03
2.0	3.31E-01	1.43E-01	1.93E-01	1.31E-01	0.00E+00	2.67E-03
4.0	2.05E-01	1.01E-01	1.50E-01	9.70E-02	0.00E+00	2.56E-03
6.0	5.17E-02	5.62E-02	4.71E-02	7.43E-02	0.00E+00	2.01E-03
8.0	1.84E-02	3.63E-02	1.93E-02	5.69E-02	4.01E-02	1.55E-03
8.7	1.39E-02	3.13E-02	1.47E-02	5.13E-02	4.05E-02	1.40E-03
10.0	8.14E-03	2.40E-02	1.24E-02	4.18E-02	4.13E-02	1.14E-03
12.0	7.85E-03	1.69E-02	5.88E-03	3.10E-02	3.74E-02	8.52E-04
14.0	7.93E-03	1.32E-02	5.28E-03	2.20E-02	2.37E-02	1.03E-03
16.0	6.35E-03	1.16E-02	5.79E-03	1.43E-02	1.70E-02	2.00E-03
19.0	1.23E-02	6.40E-03	6.25E-03	8.80E-03	1.81E-02	1.90E-03
20.0	3.42E-03	5.21E-03	5.52E-03	7.42E-03	1.64E-02	1.94E-03
22.0	5.38E-03	4.20E-03	5.92E-03	5.26E-03	2.29E-02	5.79E-03
23.8	4.31E-03	5.48E-03	5.99E-03	3.69E-03	2.29E-02	1.87E-02
25.0	3.31E-03	6.07E-03	5.82E-03	2.99E-03	2.29E-02	2.48E-02
26.7	6.23E-03	6.37E-03	8.58E-03	2.24E-03	4.75E-02	3.11E-02

[a] - days reported in terms of days and fractions of days

information on the saltcake dissolution process and any actions necessary to further process the dissolved salt solutions. The extent of channeling can be accounted for in the thermodynamic calculations.

Model Predictions for the S-109 Saturated Experiment

The S-109 tall column dissolution test conducted at ARC was a saturated test. Thus, after the simulant was prepared and added to the column in batches, the brine was allowed to drain and was recirculated to the top of the column to fully saturate and equilibrate the tall column contents prior to the addition of diluent. Once the column contents were equilibrated, 68 L of saturated brine were drained. To maintain the column under saturated conditions, only enough brine was drained to allow a level of approximately 2 cm of brine to sit atop the saltcake surface.

For the modeling of the S-109 saturated dissolution experiment, three batches of saltcake were prepared and loaded into the ARC tall column. Table VII summarizes the simulant recipe. The extent of evaporation during batch preparation as well as the transfer temperature for the three batches was consistent between batches. All three batches were combined for simulation purposes. This was possible due to the consistency of the batch preparation procedure. Input to ESP consisted of the weights of the various chemicals used to prepare the simulant. Water (258.757 kg) was removed from the simulant by evaporation and this was simulated using a component separate block. The resulting saltcake/brine stream was then equilibrated in ESP and 68 L of brine were removed, reflecting the removal of brine from the ARC tall column. Table VIII provides a summary of the amounts of each ion removed during the draining of brine. Both experimental and simulation results are reported.

The differences noted in the initial amounts for sodium and aluminum in the experimental and final results are due to the molecular formula used for the input sodium aluminate. Technical grade sodium aluminate has the molecular formula of $NaAlO_2 \cdot 2H_2O$. Thermogravimetric analysis (TGA) and Inductively Coupled Plasma (ICP) analysis was performed on a sample of the sodium aluminate used by ARC, with the resulting molecular formula, $0.5785NaAlO_2 \cdot 0.0484Al(OH)_3 \cdot 0.2171NaOH \cdot 0.17H_2O$. This was used for the evaluation of initial amounts of each ion for the ESP prediction, but the experimental data from ARC were not changed to reflect this more accurate molecular formula. Similarly, the molecular formula for sodium phosphate employed by ARC was taken as $Na_3PO_4 \cdot 0.25NaOH \cdot 12H_2O$. For the major species, sodium and nitrate, the amounts removed during brine drainage were consistent between the experimental results and the ESP predictions. For the majority of species, the predicted amount of a particular ion removed from the column as a result of brine drainage was different from the experimental value by no more than approximately 0.5 kg. The predicted %-removed for the majority of species was also in good agreement. The height of the saltcake column was estimated from the ESP results using the density and mass of brine retained along with the solid phase speciation and component densities. The predicted height was 218.4 cm compared to the experimental value of 215.4 cm.

The dilution portion of the experiment was modeled in discrete intervals. Each interval was specified based on data supplied by ARC regarding diluent addition and cumulative volume removed as effluent. Each interval was modeled using three ESP blocks: 1) MIX block – diluent was added to the solid and the retained brine from the previous interval; 2) SEP block – the

equilibrated liquid brine was separated from the solid saltcake; and 3) SPLIT block – the liquid brine was partitioned into removed brine and retained brine streams. For each interval, the experimental amount of diluent added was introduced to the MIX block. The experimental amount of effluent removed during the interval was used to control the stream partitioning in the SPLIT block. A total of twelve intervals were used, encompassing the experiment timeline of approximately 80 days. The saltcake and retained brine were used to estimate the height of the column contents at each interval. Estimated heights were compared to the experimental data. For each interval, an average concentration in g/L was computed from the raw data supplied by ARC. These averages were compared to the ESP prediction of ion concentration for each interval. The liquid effluent density predicted by ESP was also compared to available specific gravity data from ARC. The saltcake column height and the density comparisons are shown in Fig. 4.

Table VII. Simulant Recipe for S-109 ARC Tall Column Saturated Test (all masses in kg)

Compound	Batch 1	Batch 2	Batch 3	Total
$NaAlO_2 \cdot 2H_2O$	3.810	3.350	2.907	10.067
NaOH	0.250	0.250	0.224	0.724
Na_2CO_3	4.900	4.880	4.199	13.979
$Na_2C_2O_4$	0.480	0.470	0.405	1.355
NaPHOH[a]	5.680	5.610	4.832	16.122
Na_2SO_4	1.370	1.370	1.184	3.924
NaF	0.070	0.070	0.060	0.200
NaCl	0.140	0.120	0.112	0.372
$NaNO_2$	1.300	1.300	1.120	3.720
$NaNO_3$	96.980	96.970	83.506	277.456
H_2O	120.540	120.040	103.438	344.018

[a] NaPHOH = $Na_3PO_4 \cdot 0.25NaOH \cdot 12H_2O$

One interesting feature of the height profile as a function of time is the small dip in the column height during the initial stages of the experiment. During the first interval, a total of 20 L of diluent was added while 30 L of effluent were drained from the column. For the second interval, the diluent addition at 30 L was balanced by effluent withdrawal of 31 L. During the third interval, 30 L of diluent were added, but only 20 L of effluent withdrawn. By using these amounts for diluent addition and to partition the brine stream for effluent removal in the ESP simulation, the general behavior of the height as a function of time in the early stages of diluent addition was captured. The estimated column height was in good agreement with the experimental height measurements until the total height reached approximately 50 cm. To estimate the combined height of the saltcake and brine in the column, the solids volume and the brine volume were used, assuming that there were no voids within the bed, or pores that were not filled with brine. This is a conservative estimate, particularly in the later stages of the experiment, when the majority of the easily dissolved salts have already been removed from the column through dissolution. Those solids that remain are in the saltcake, predicted to be primarily gibbsite and sodium oxalate, may form a porous structure with some pores not fully filled with brine. This porous structure was not accounted for in the estimation of saltcake height from ESP results. Also shown on Fig. 4 is a comparison of the predicted liquid effluent density

and the experimental density averaged for each time interval. Again, ESP predictions track the experimental data quite well.

Shown in Fig. 5 are the concentration profiles for sodium and for nitrate, the two major constituents in the S-109 simulant recipe. The full set of experimental concentrations from ARC are plotted along with the averaged concentration for each time interval and the ESP prediction for the ion concentration. The general trends for both nitrate and sodium ions are well predicted by the ESP model. Predicted trends for components present in lesser amounts (not shown here) were also in general agreement with the experimental data.

Table VIII. Summary of % Ion Removed During Draining of Brine for S-109 Saturated Test

Species	ARC Experimental Results			ESP Prediction		
	Initial (kg)	Final(kg)	% Removed	Initial (kg)	Final(kg)	% Removed
Na^{+}	90.542	75.76	16	90.772	75.466	16.9
Al^{3+}	3.161	2.85	10	2.705	2.114	21.9
F^{-}	0.09	0.09	1	0.085	0.082	3.7
Cl^{-}	0.226	-0.004	102	0.226	0.100	55.5
NO_2^{-}	2.48	1.166	53	2.48	1.104	55.5
NO_3^{-}	202.408	181.699	10	202.408	179.362	11.4
PO_4^{3-}	3.927	3.545	10	3.925	2.186	44.3
SO_4^{2-}	2.654	1.428	46	2.654	1.181	55.5
$C_2O_4^{2-}$	0.89	0.412	54	0.89	0.875	1.7
CO_3^{2-}	7.915	4.59	42	7.915	5.276	33.3

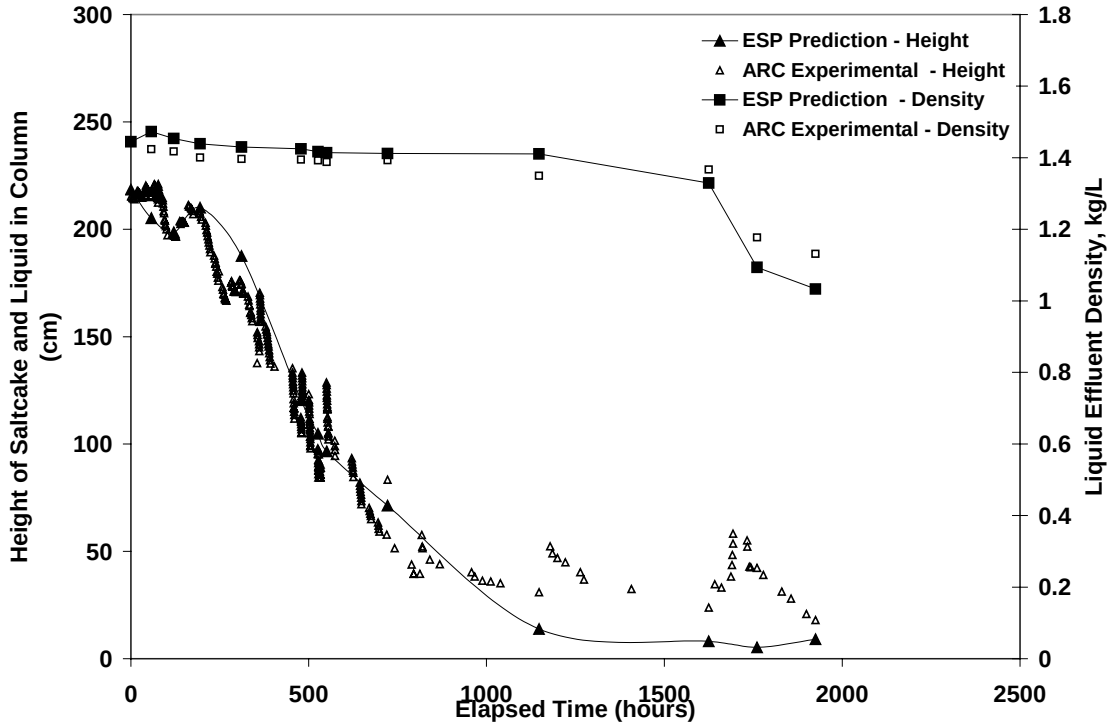

Fig. 4. Comparison of saltcake height and liquid effluent density for S-109 saturated dissolution test

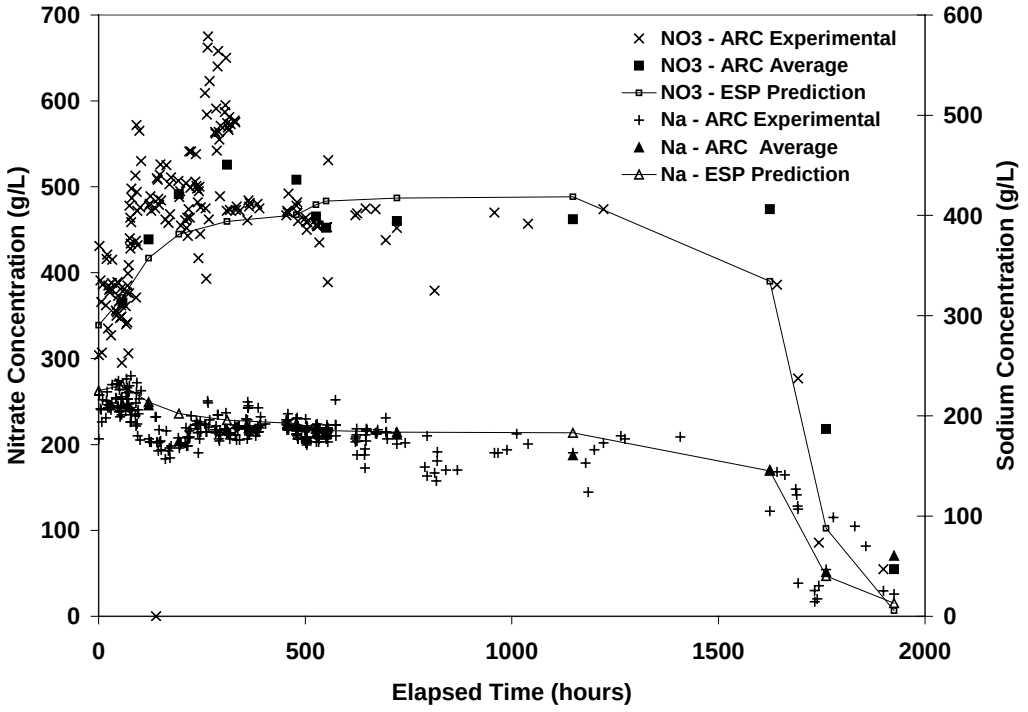

Fig. 5. Comparison of Sodium and Nitrate ion concentrations for S-109 tall column saturated test

CONCLUSION

Additional model validation data have been obtained by comparison of the ESP results with the pilot-scale dissolution experiments conducted at ARC. These calculations have provided valuable insight into developing and executing model flowsheets that can ultimately be employed for estimating concentration ranges during actual retrieval operations. The flowsheets can be applied to evaluate the extent of channeling or water bypass through the salt matrix and, using the frameworks described, can be performed prior to a scheduled retrieval. Modeling of the S-109 saturated test was straightforward. The consistency in batch preparation between the three batches of simulant prepared allowed the entire saltcake column to be modeled as a single entity. Further comparison of the ESP model with additional large-scale saltcake dissolution experiments conducted at ARC are in progress.

REFERENCES

1. Reynolds, D.A., (1995), *Practical Modeling of Aluminum Species in High-pH Waste*, WHC-EP-0872, Westinghouse Hanford Company; Richland, WA.
2. Herting, D.L., Lunsford, T.R., (1994), *Significant Volume Reduction of Tank Waste by Selective Crystallization: 1994 Annual Report*, WHC-SD-WM-TI-643, Rev 0., Westinghouse Hanford Company; Richland, WA.

3. Kirkbride, R. A., et al., (2005), *Hanford Tank Waste Operations Simulation Model Data Package for the Development Run for the Refined Target Case*, RPP-RT-23412, Rev 0A, CH2M Hill Hanford Group, Richland, WA.
4. Thompson, L. E., et al., (2003), *Development of the Bulk Vitrification Process for the Low Activity Fraction of Hanford Single Shell Tank Wastes*, Waste Management 2003 Symposium, Tucson, AZ.
5. Herting, D. L., (2000), *Saltcake Dissolution FY 2000 Status Report*, HNF-7031, Fluor Hanford, Richland, WA.
6. Toghiani, R. K, Lindner, J. S., (1999), *Saltcake Dissolution Modeling, FY 2000 Status Report*, DIAL-40395-TR00-1, Diagnostic Instrumentation and Analysis Laboratory, Mississippi State University, Mississippi State, MS.
7. Antonyraj, A., Durve, T., Toghiani, R.K., Lindner, J.S., Hunt, R.D., (2003), *Saltcake Dissolution Studies in Support of Single-Shell Tank Retrieval*, Waste Management'03, Tucson, AZ.
8. Smith, L. T., Lindner, J.S., Toghiani, R.K., Antonyraj, A., Phillips, V.A., (2005), *Modeling and Experiments for the SRS Low-Curie Salt Process*, paper presented at the 14th Symposium on Separation Science and Technology for Energy Applications, Gatlinburg, TN, submitted to *Separation Science and Technology*.
9. Ebadian, M. A., et al., (2003) *High-Level Waste Saltcake Dissolution Studies" FY 2003 Year-End Report*, Florida International University, Miami, FL.
10. Philippidis, G., (2004) *High-Level Waste Saltcake Dissolution Studies: 2004 Technical Progress Repor*t S-109 Saturated.
11. <http://twins.pnl.gov:8001/twins.htm>, accessed .
12. Hunt, R. D. email communications 2003, 2003.
13. Jung, Mi-Hee, (2005) *Thermodynamic Solubility Studies on $NaAlO_2$-$NaNO_3$-OH System to Remove Aluminum Compounds in Nuclear Waste*, M.S. Thesis, Chemical Engineering, Mississippi State University, Mississippi State, MS.
14. Dodson, M. G. et al., *Selection of At-Tank Analysis Equipment for Determining Completion of Mixing and Particle Concentration in Hanford Waste Tanks*, PNNL-12223; EW4010, Pacific Northwest National Laboratory, Richland, WA.